RADIOGRAPHIC FACILITY IN INS ŚWIERK

J. Bigolas, W. Drabik, E. Pławski, A. Wysocka

The Andrzej Soltan Institute for Nuclear Studies
05-400 Swierk/Otwock, Poland

plawski@ipj.gov.pl
wysocka@ipj.gov.pl

Department of Accelerator Physics and Technology

View of experimental hall with radiation protection

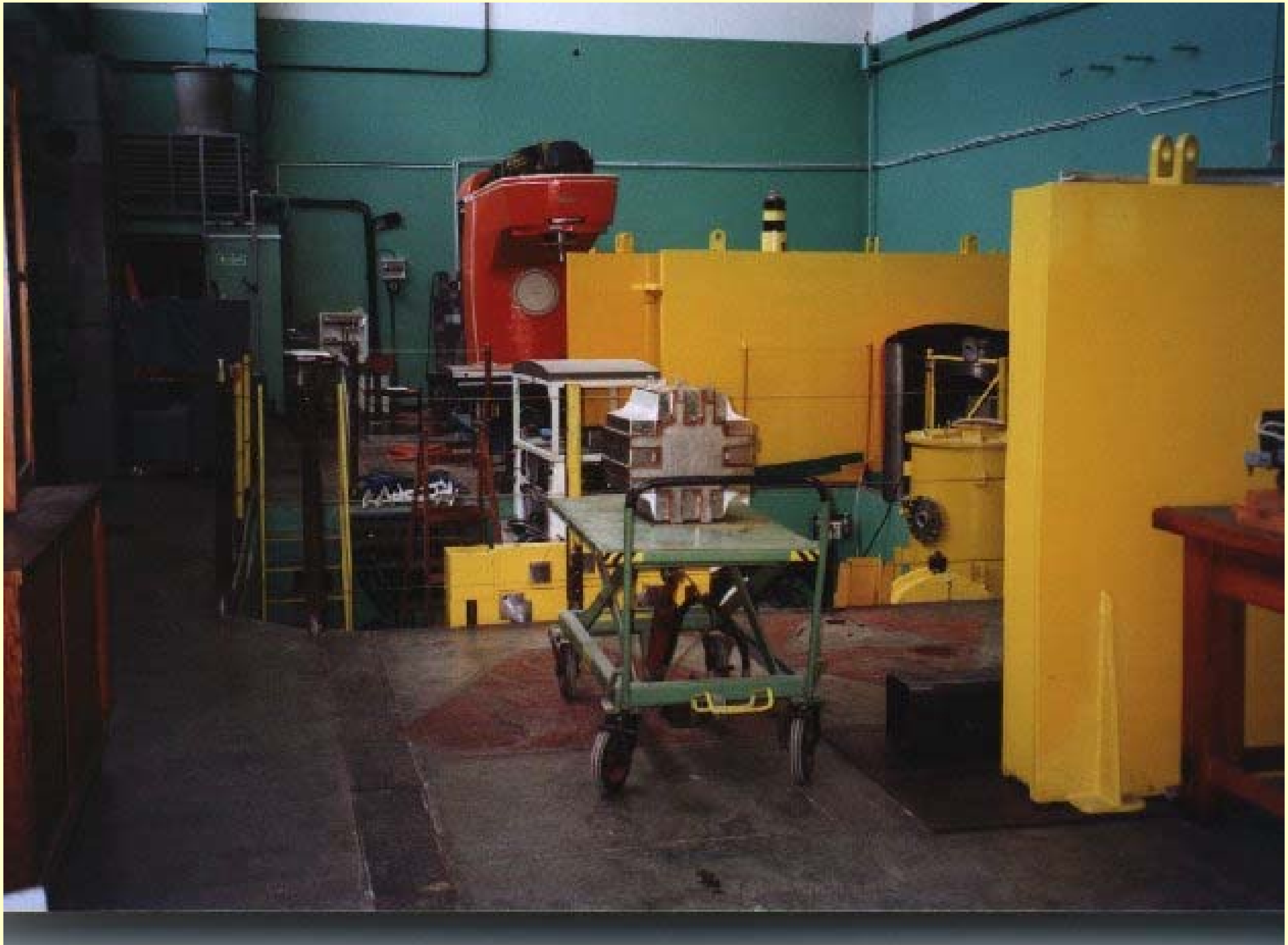

,

Cyclotron for radioisotope production; protons 15-30MeV, isochronic, 4 sectors, 18 kGaus,RF 53 MHz, diameter 105 cm

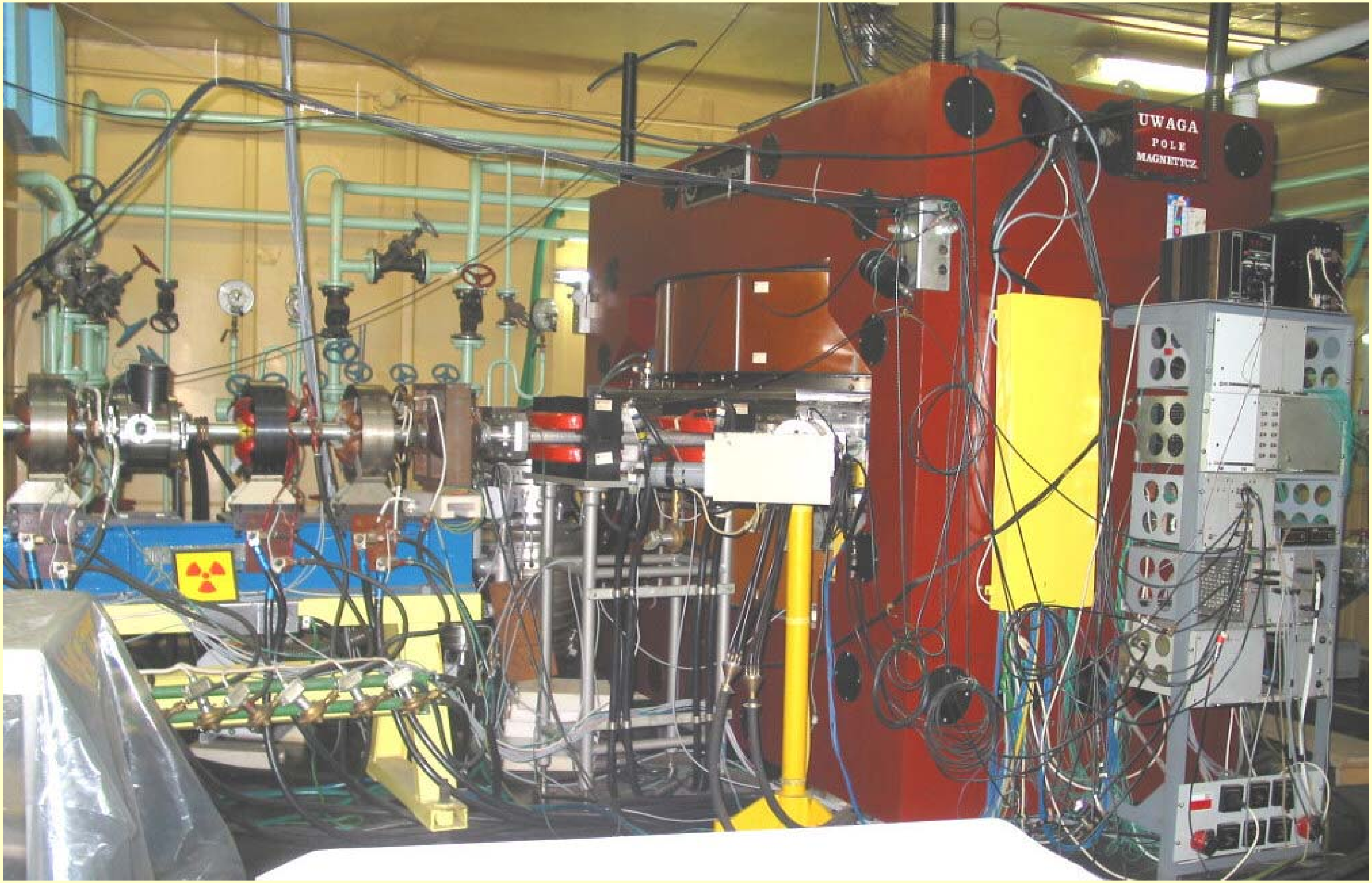

,

Model of a superconducting super-structure – TESLA

DESY collaboration

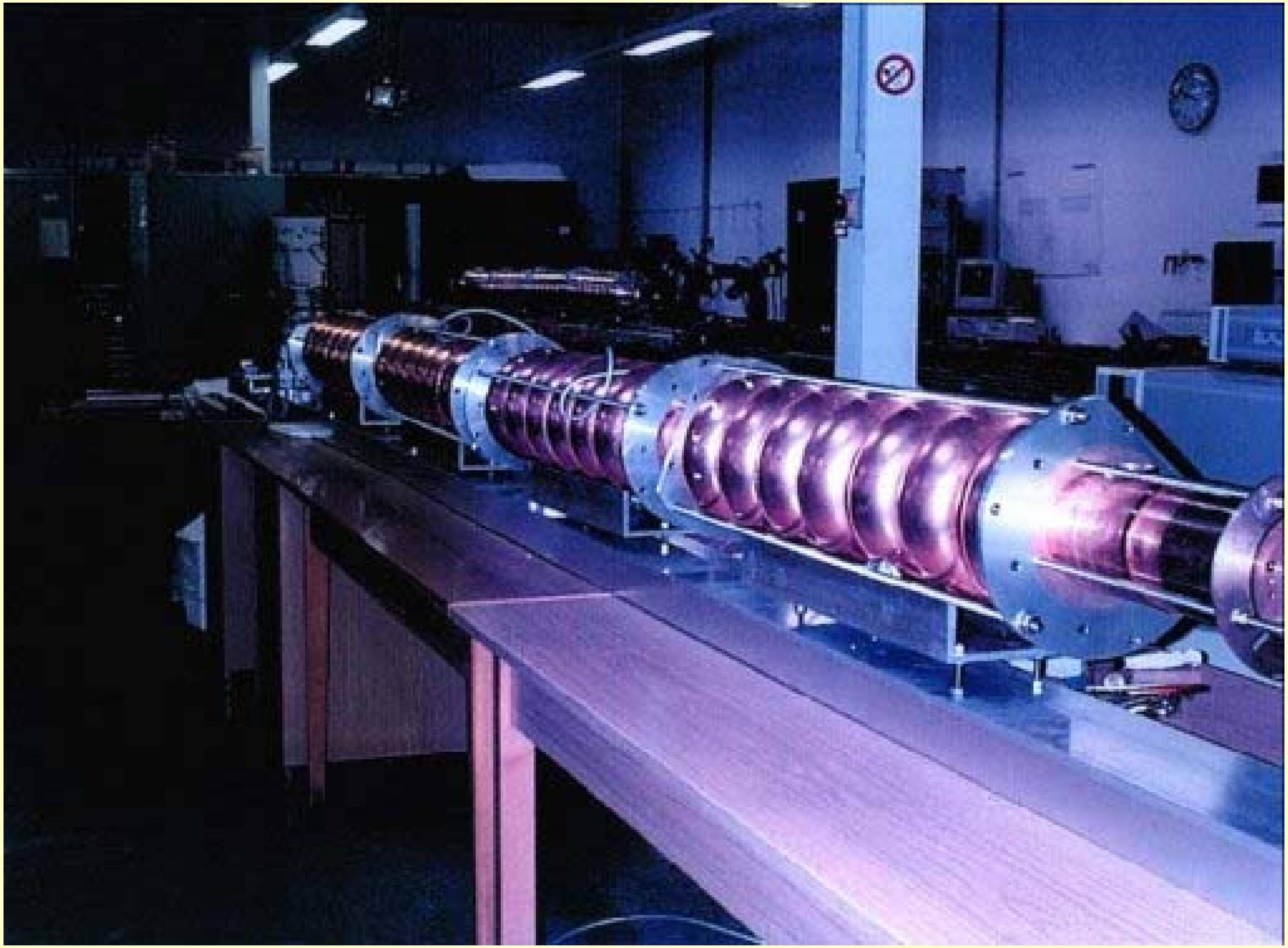

,

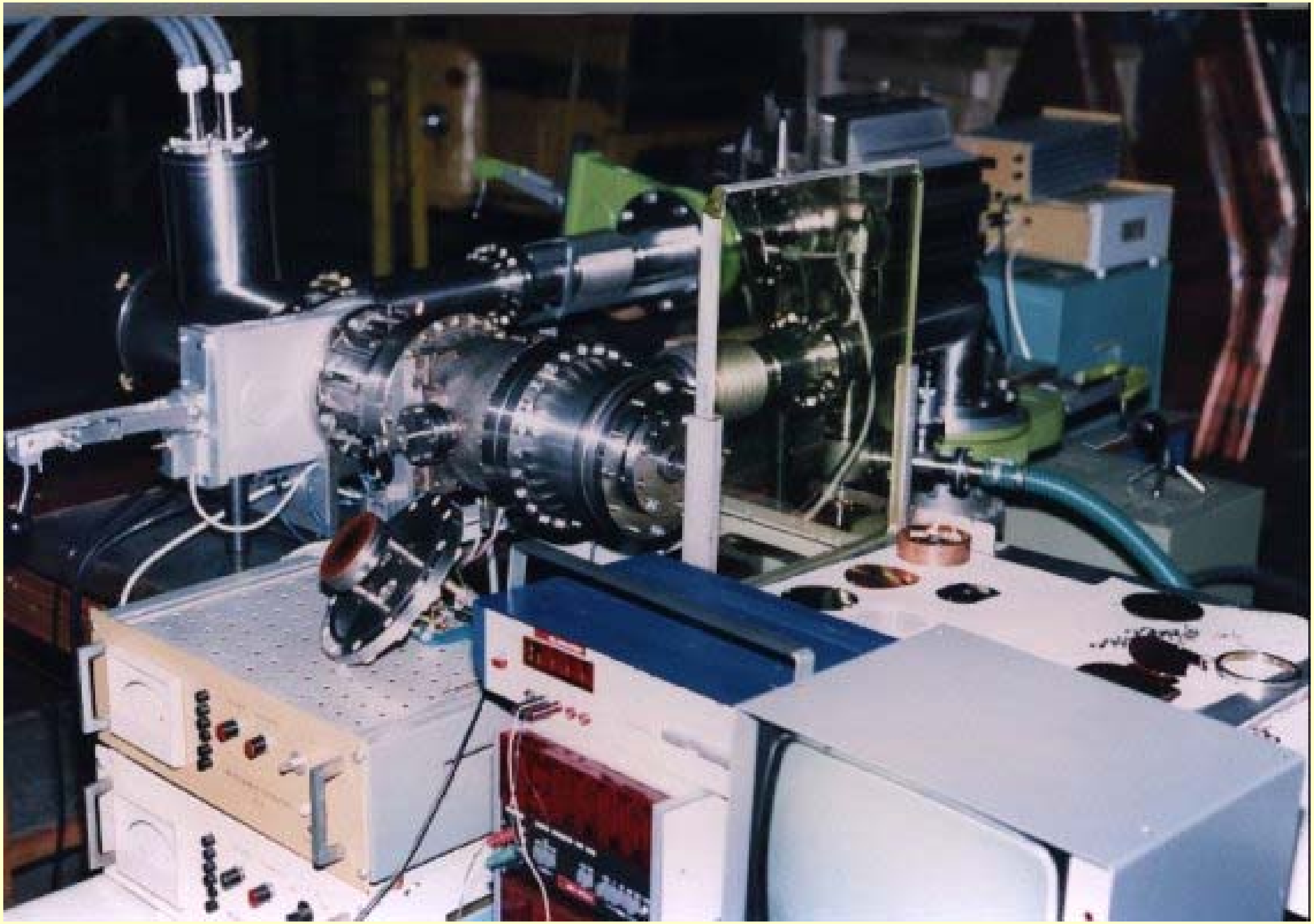

High power electron source elaborated for Sincrotrone Trieste;

E=20keV, i=200mA

Contents

•Introduction

•The Design of the Accelerator

Design Calculations and Optimisation
RF Accelerating Structure and Auxiliaries
Electron Beam Spectra Measurements

• Monte Carlo Calculations of the Photon Beam

• The Radiographic Pictures

,

Introduction:electron accelerator and e-X conversion units

- The 6 MeV linac electron accelerator can work in the electron mode and in the X-ray photon mode. Especially the photon beam may be used for radiographic non-destructive investigations on laboratory scale and after some modifications for industrial purposes.
- The linear RF accelerating structure composed of 11 on axis coupled cells is working in S band on the frequency 3 GHz.
- The accelerated electron beam passes into air through thin (40 μm stainless steel) vacuum window
- The water-cooled, removable e/X conversion head holding tungsten target can be placed few millimetres downstream this window.Target thickness is 1 mm.

,

electron accelerator and e-X conversion units

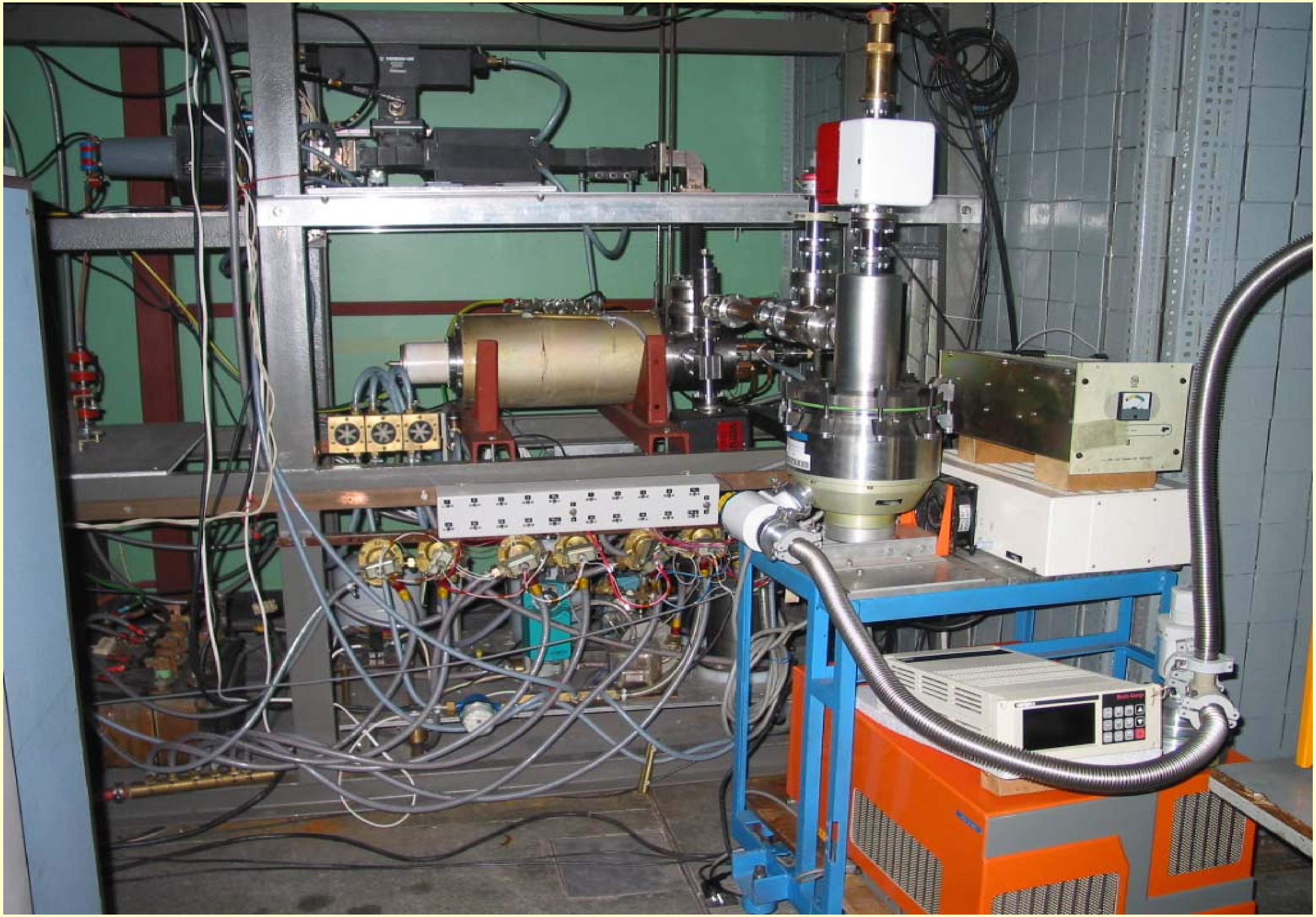

1. electron gun; 2.accelerating structure 3.RF power source (magnetron), circulator (protection of the magnetron against reflected wave)

Design Calculations and Optimisation

Construction of accelerator was preceded by a thorough computational optimisation of the electron gun and successive RF accelerating structure.

The computational codes:

”E-Gun Code”, SLAC and “Poisson-Superfish” Los Alamos, were checked by beam dynamics codes developed in our Institute in order to obtain the optimum shapes of structures.

The samples of final computational results are presented in the following figures

,

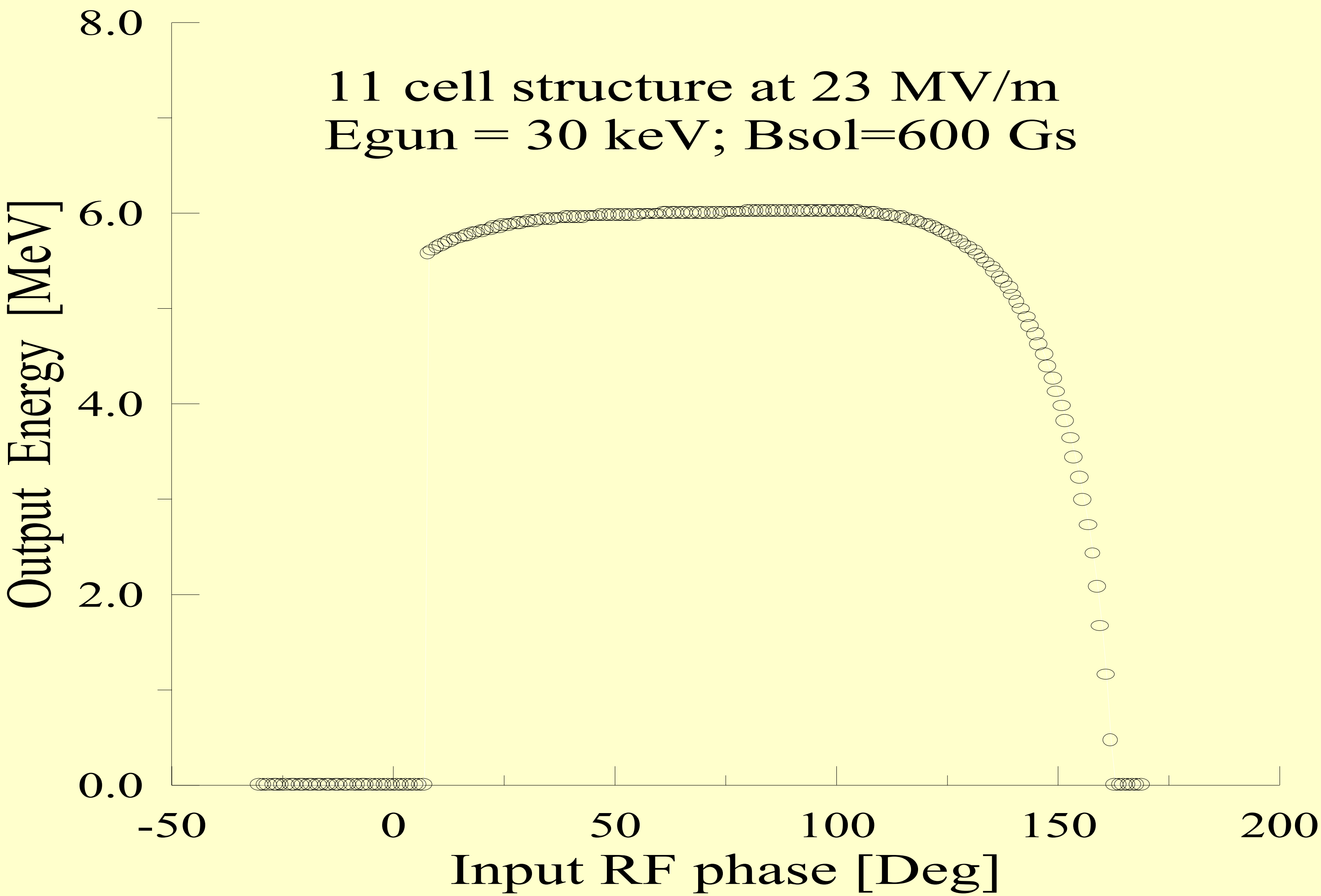

Computed phase acceptance of accelerating structure.

23 MV/m amplitude corresponds to 15 MV/m mean field

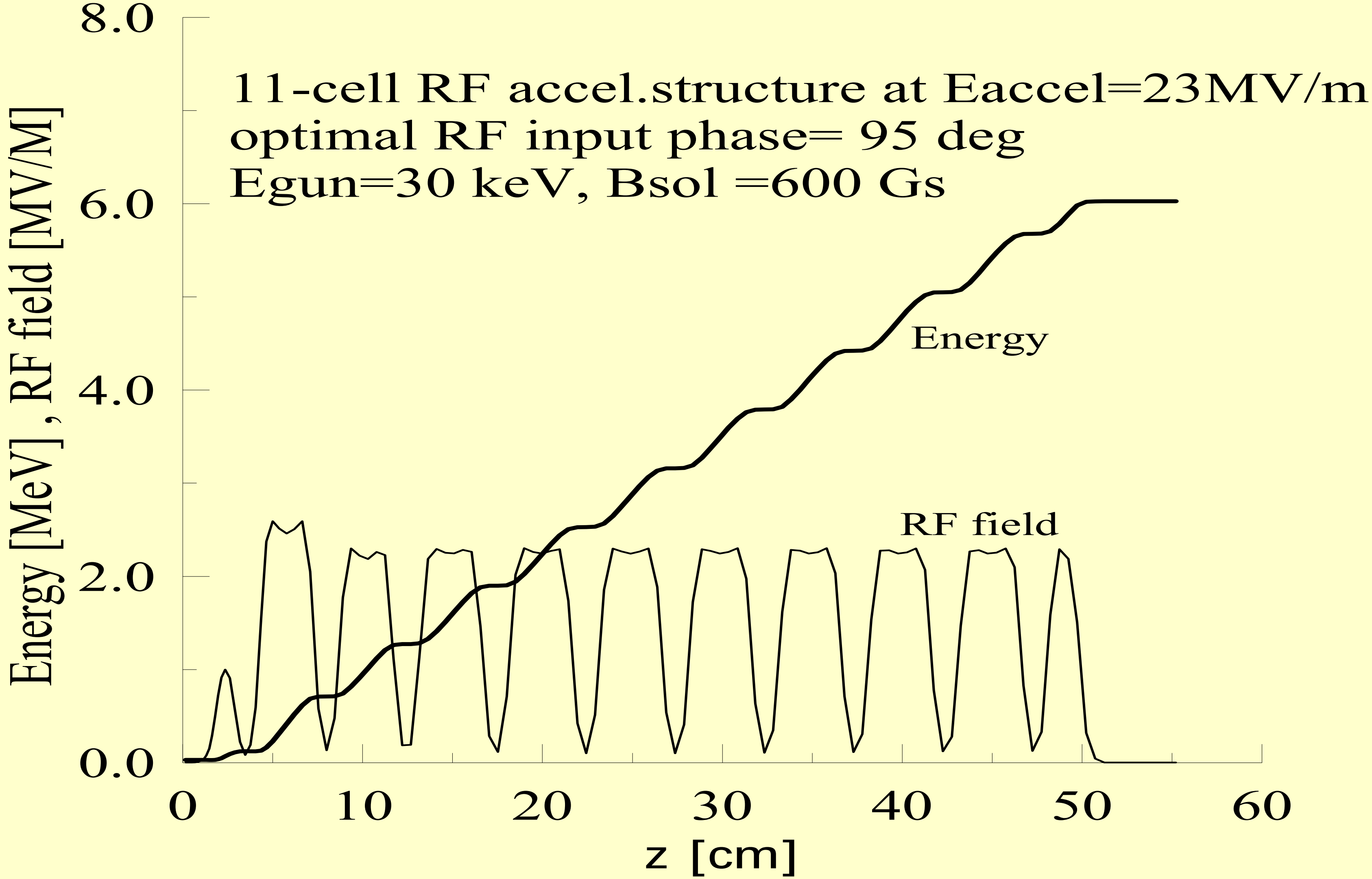

Electron beam transmission through RF accelerating structure at optimal input phase 95^0 RF

,

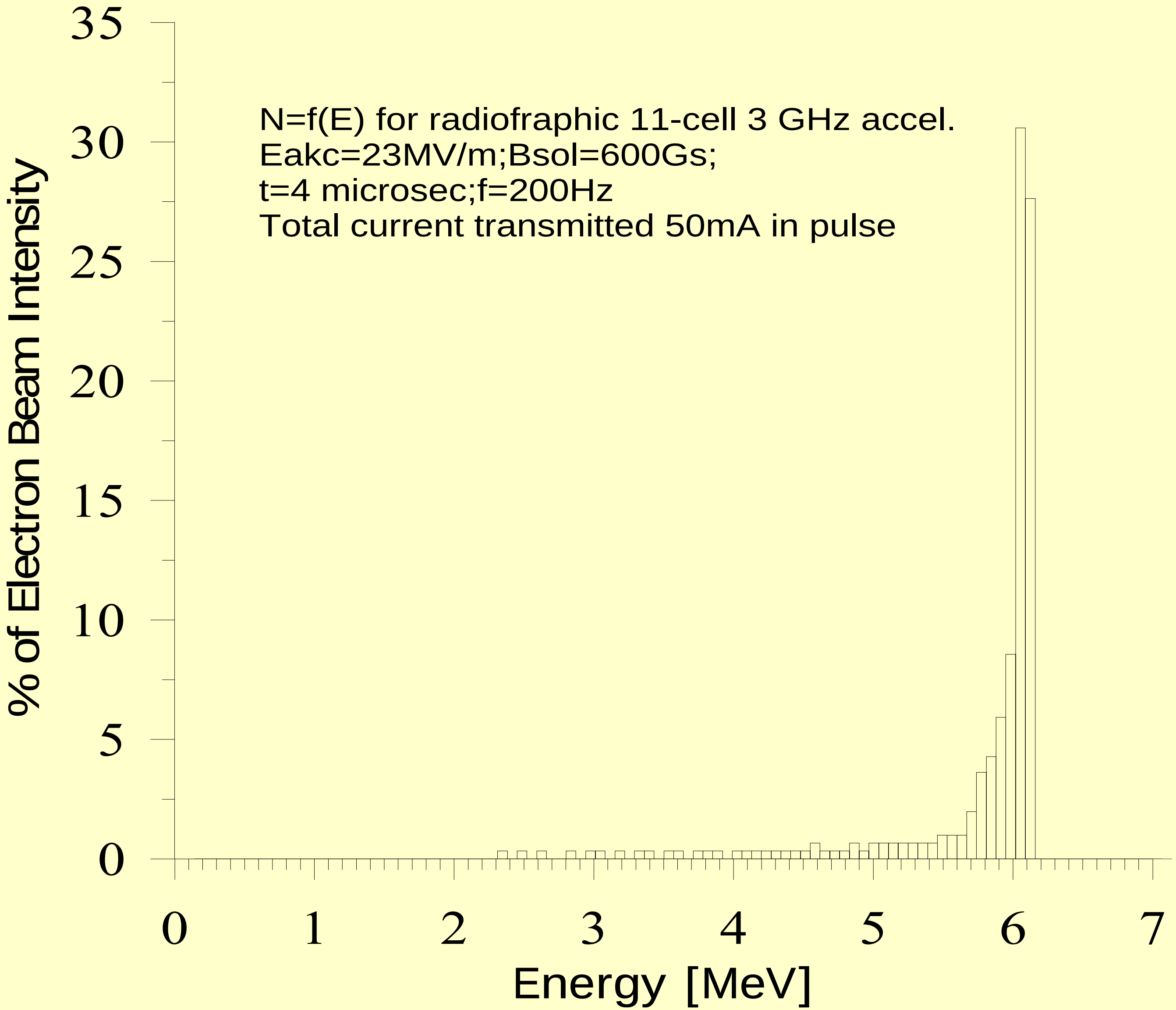

Calculated electron energy spectrum on W target of radiographic 6 MeV accelerator

A block diagram of the radiographic facility

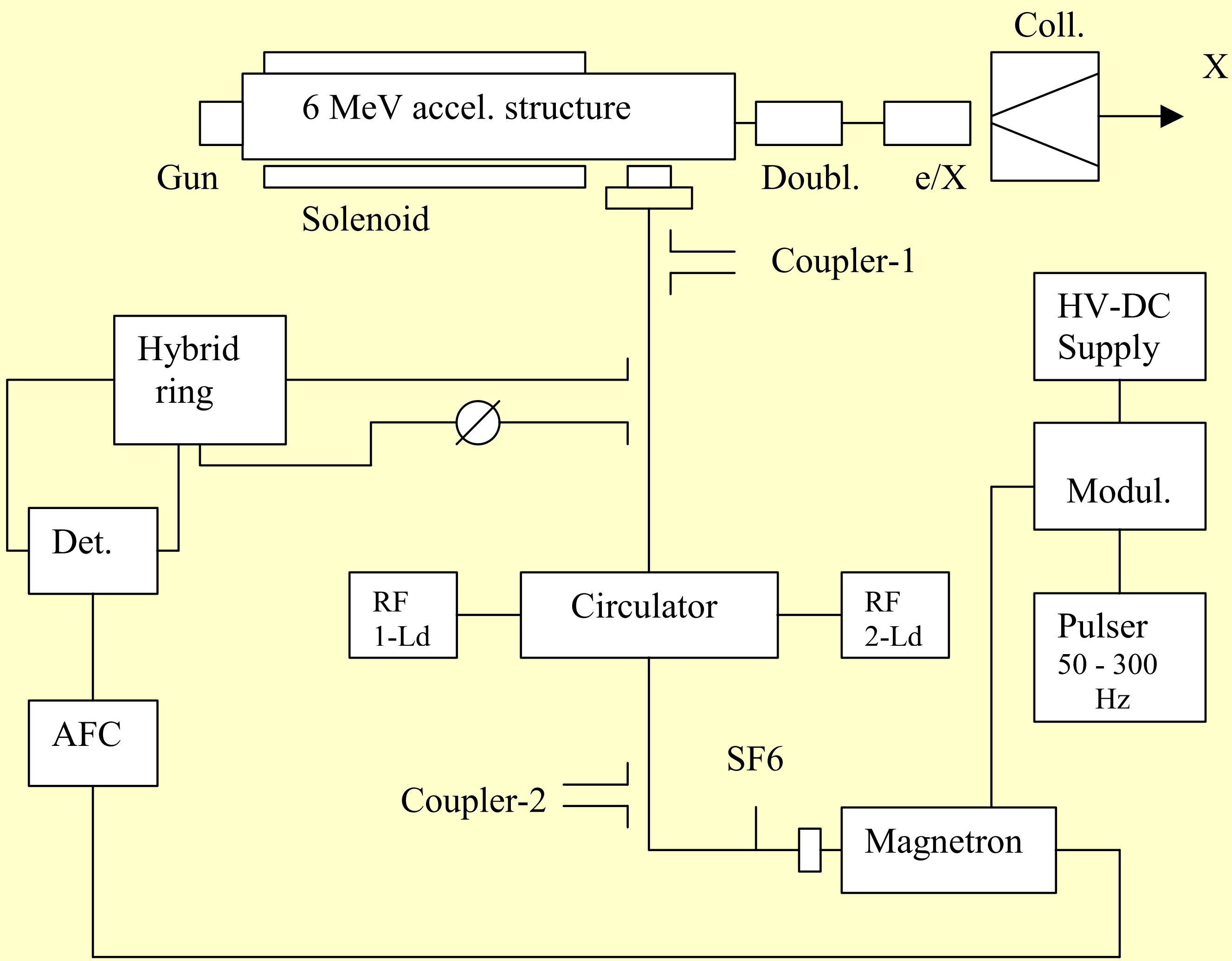

- The RF power-exciting electromagnetic field in the accelerating structure is generated by a 2999 MHz, 2 MW in-pulse magnetron, and is delivered to the coupling window of the accelerating structure via a pressurised WR284 waveguide system.

- This system consists of a 4 -way circulator, RF power loads and various RF sensing and regulation devices, as also shown in the last figure.

- An automatic frequency tuning (AFC) system tunes the magnetron to the structure frequency.

The basic components and parameters of accelerator(1)

1. Electron gun

- electrons are injected from thermionic diode gun pulsed together with RF power source exciting the accelerating structure
- Diode, cylindrical Pierce geometry type, thermionic tungsten cathode,
- Energy/Intensity : 30keV/ 200mA in pulse 4 μsec ; variable repetition 50-300 Hz

The basic components and parameters of accelerator(2)

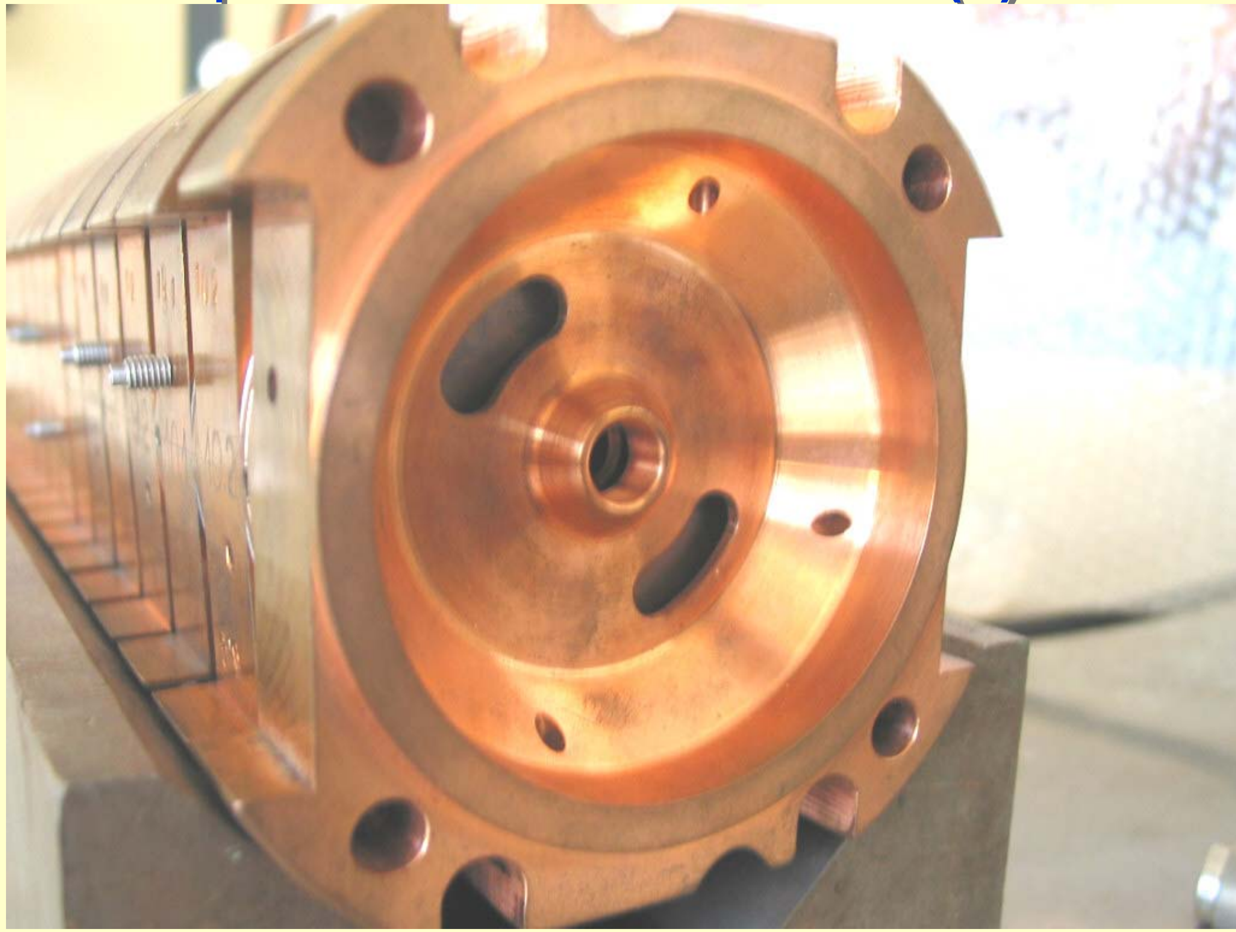

2.RF accelerating structure

-linear RF accelerating structure composed of 11 on axis coupled cells working in S band on the frequency 3 GHz. It is excited in the so called $\pi/2$ mode

-Nominal energy : 6 MeV ; Electron current : 100 mA in pulse, 0.1 mA average

-Structure length (total) : 50 cm ; Working temp. 40 ± 1 ºC **,** Quality factor: 12 500

RF Accelerating Structure and Auxiliaries

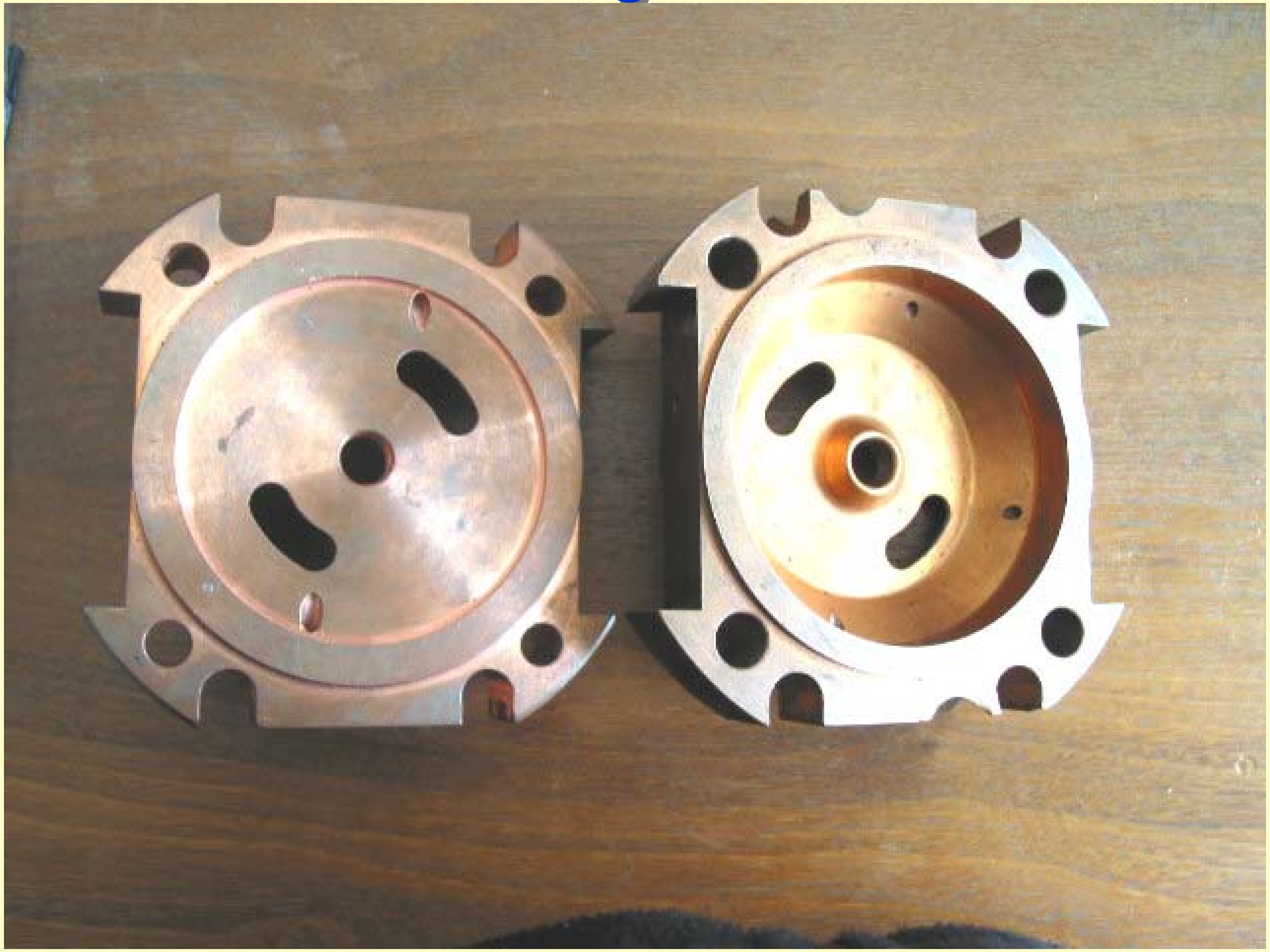

Components of the RF accelerating structures are fabricated from certified OFHC copper. Two fabricating options are available: brazing in a vacuum or brazing in hydrogen atmosphere.

In the first case, the grain size of copper is more critical, while in the second the content of oxygen is very important. The structure actually mounted in radiographic facility was brazed in vacuum oven. After the last brazing operation, the whole structure was finally tuned to the working $\pi/2$ mode

,

The basic components and parameters of the Accelerator (3)

3. Beam Focusing

- Solenoid surrounding the accelerating structure

- Maximum attainable axial magnetic field 700 Gs

- Magnetic quadrupole doublet on structure output

- Beam position correctors: two pairs of small coils between the structure and the solenoid coil

Quadrupole doublet

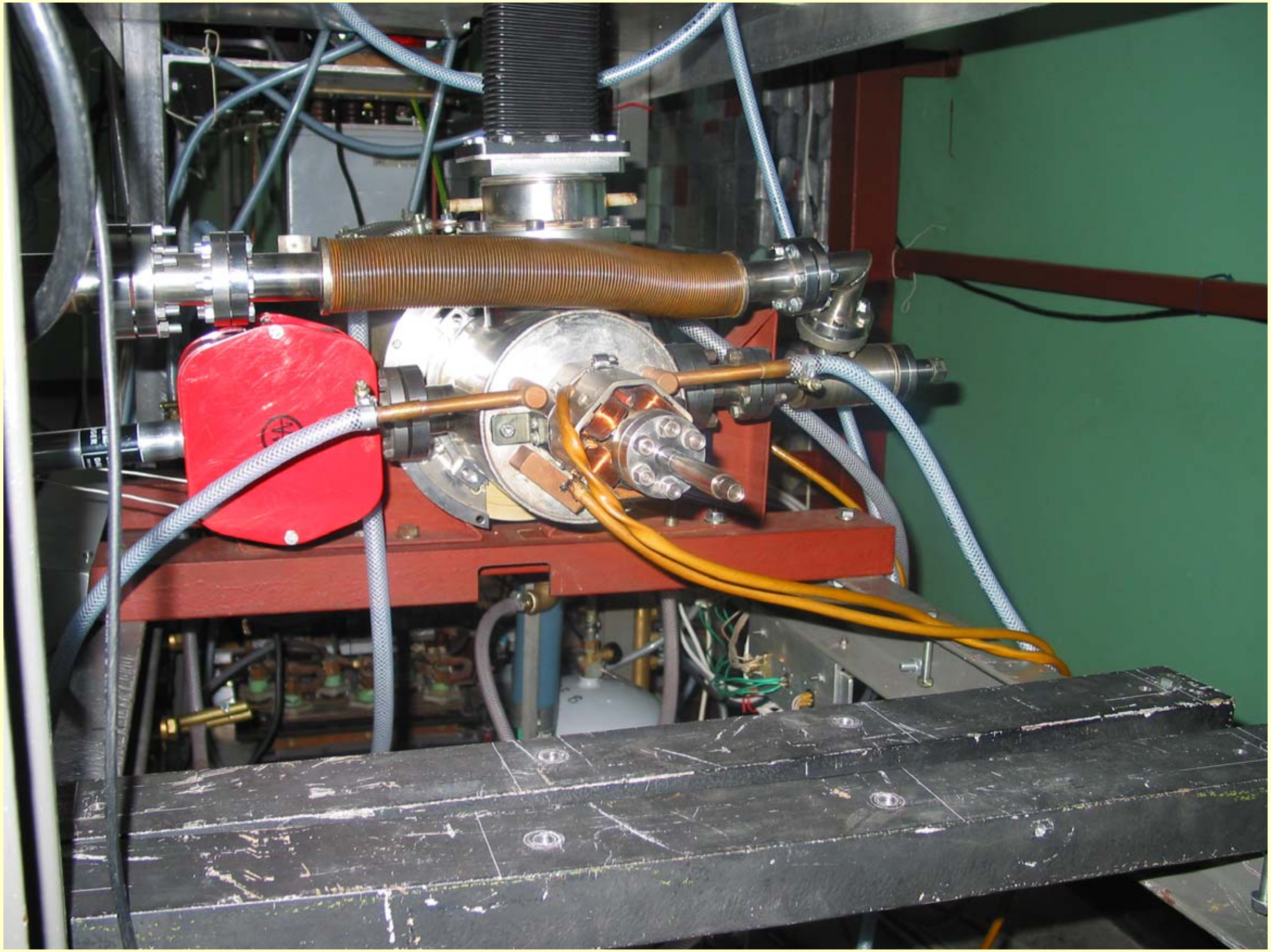

Electron beam

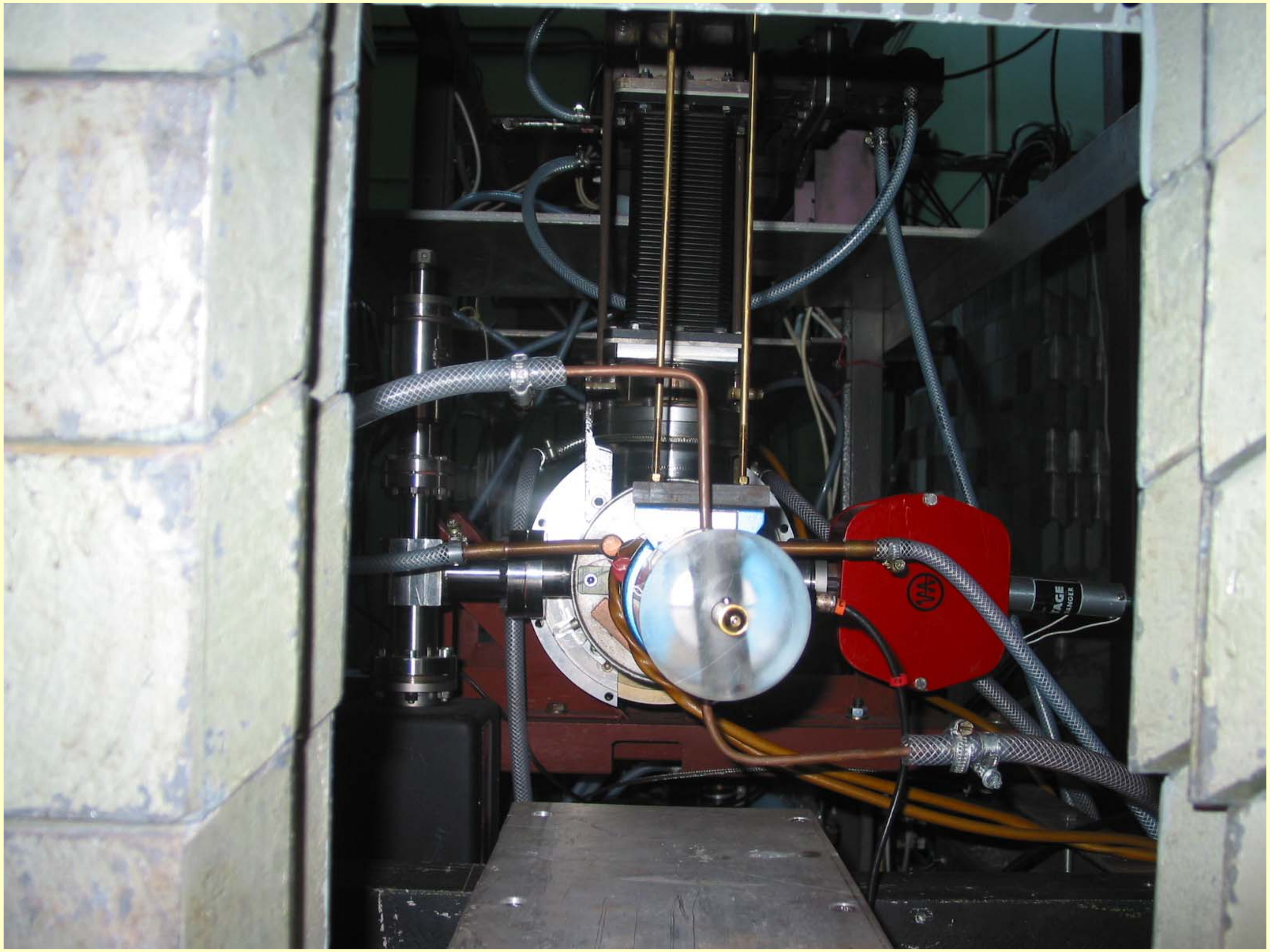

collimator

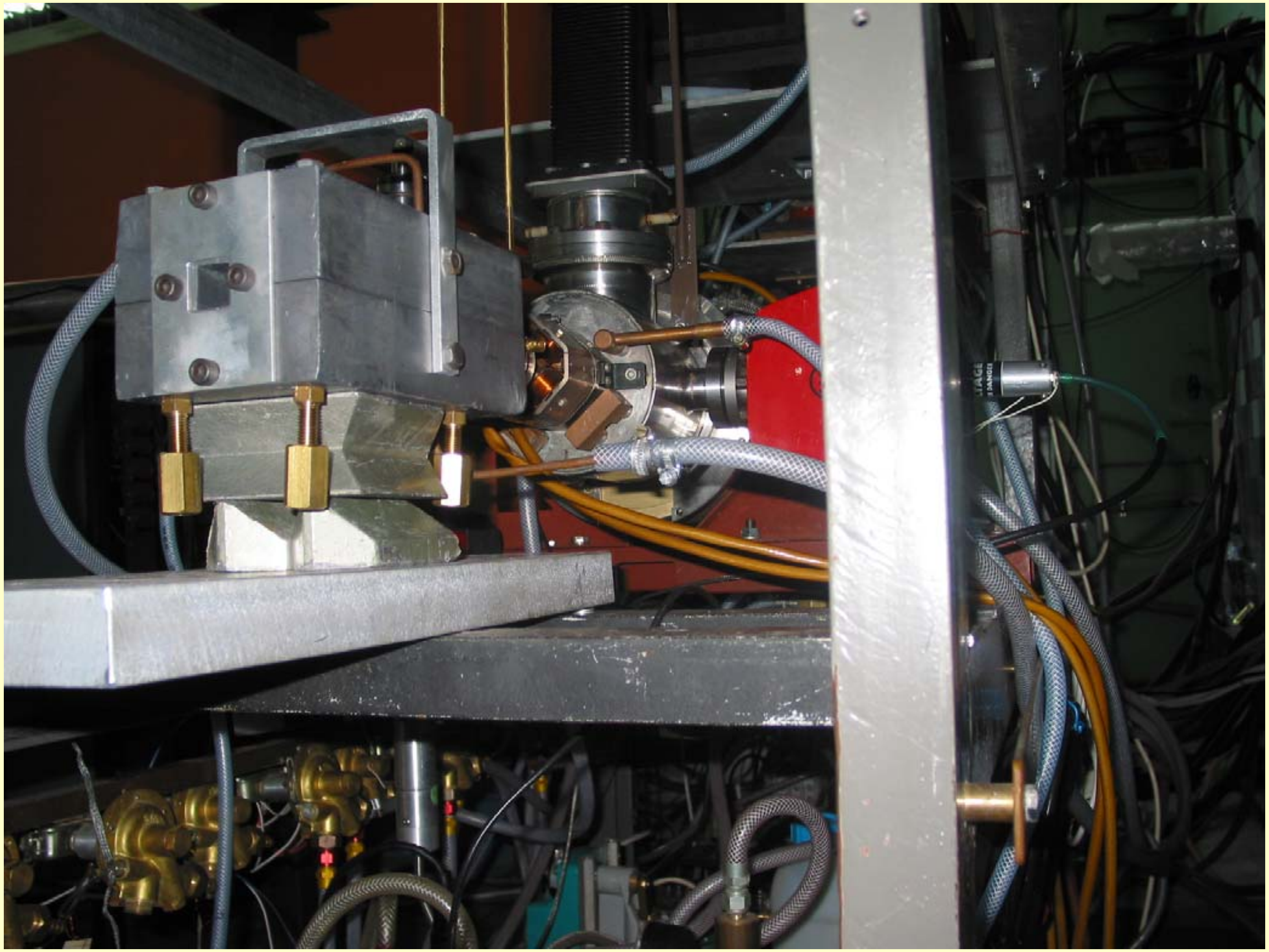

Electron Beam Spectra Measurements

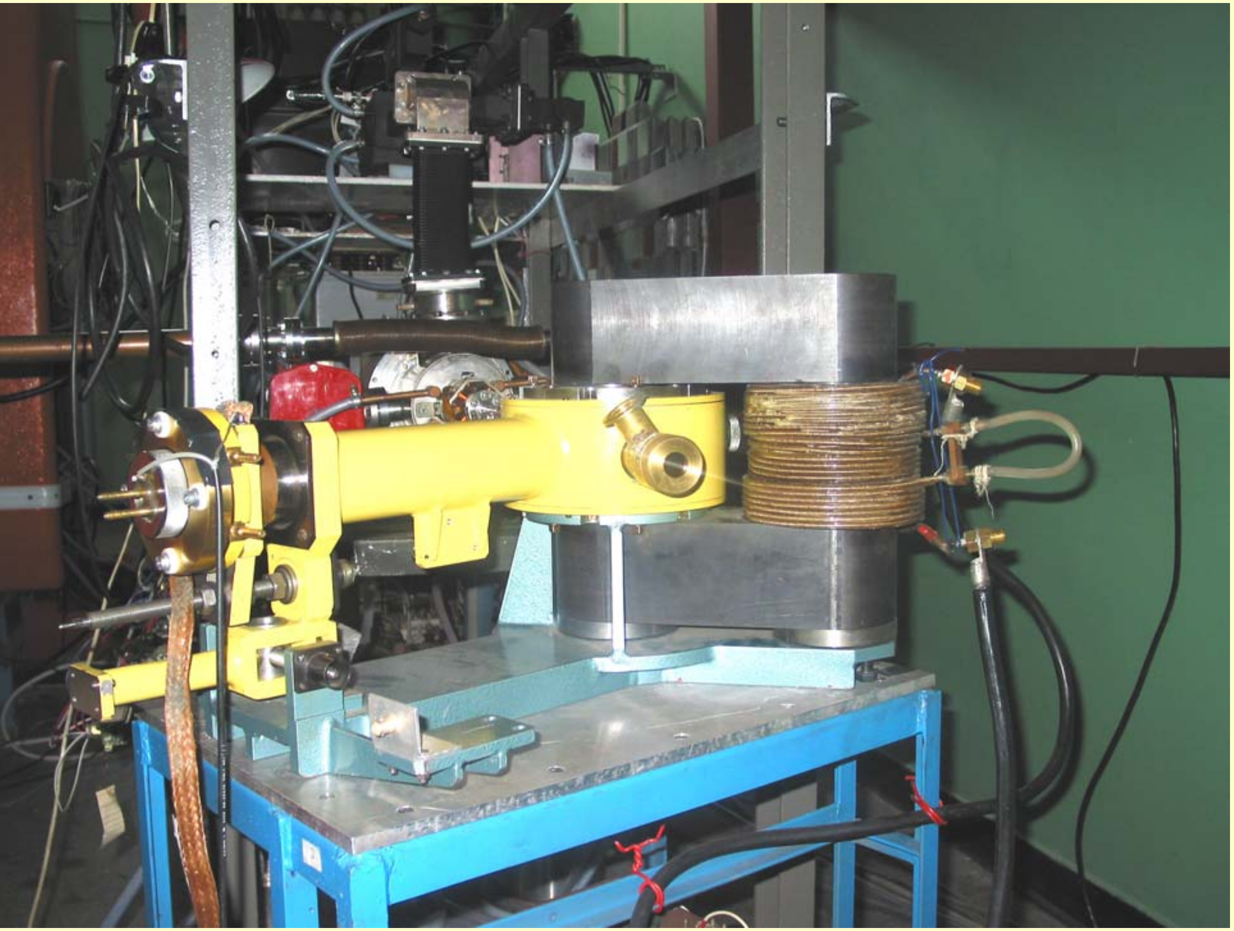

In the electron mode, measurements of the electron beam spectra were made using a simple magnetic analyser. The electron beam emerging form the accelerating structure is deflected in the magnetic field of the analyser by 60 degrees.

Then, after passing through the energy defining slit, it is collected in the Faraday cup. The current of the Faraday cup is converted to a voltage signal and measured with an oscilloscope.

Electron Beam Spectra Measurements

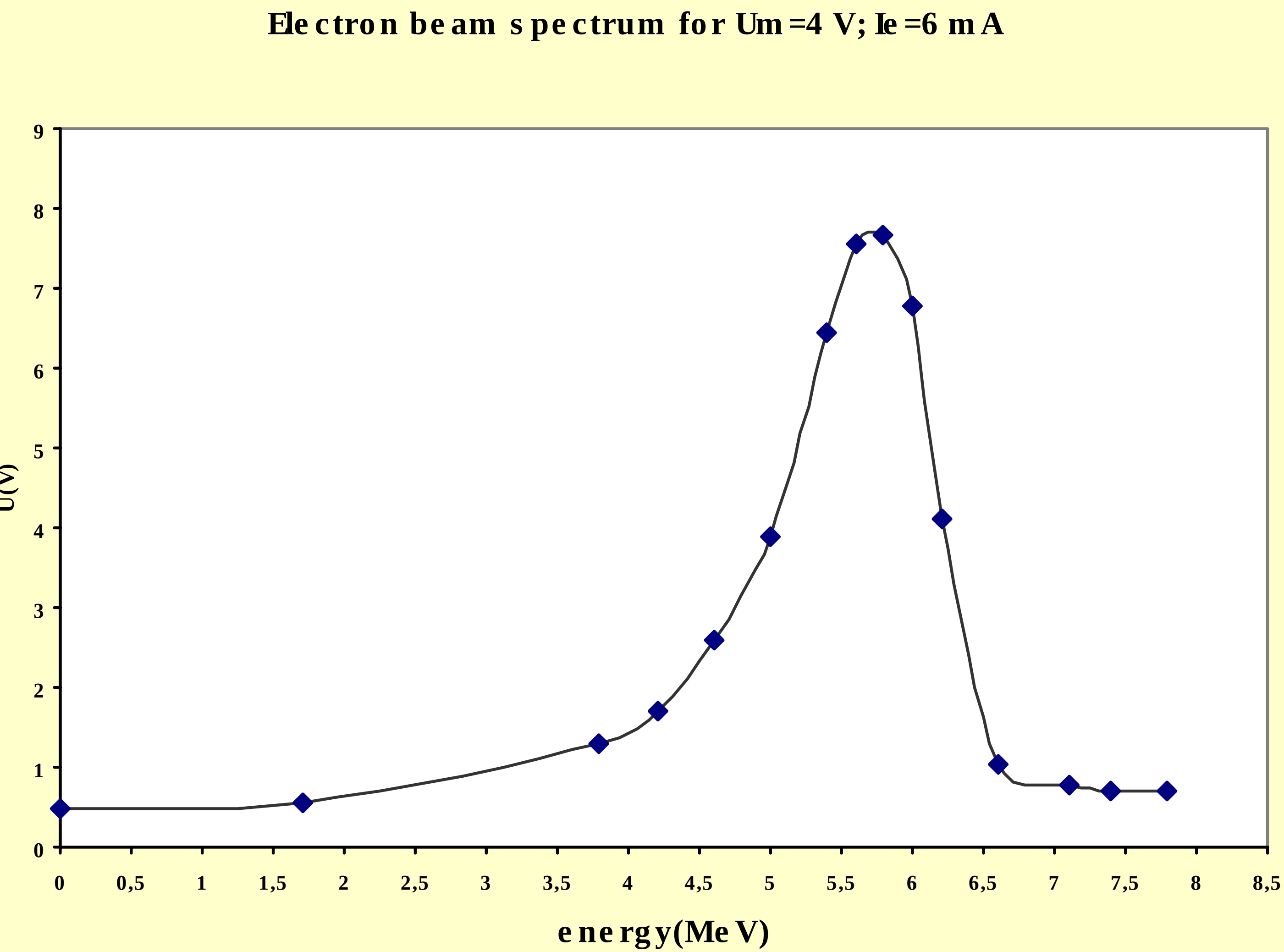

- The electron beam energy was determined from relationship between magnetic field intensity and energy.
- The result was verified by calculations of electron beam trajectories in the magnetic gap taking into account fringe effects .

,

Monte Carlo Calculations of the Photon Beam (1)

•code BEAMnrc/EGSnrc, was used to calculate spectral distribution, mean energy distribution and fluence versus position for a photon beam

•for 7 x 10^7 particles, using an electron transport cutoff of ECUT=0.7 MeV, and a photon transport cutoff of PCUT=0.01 MeV.

•the maximum fractional electron energy loss per step (ESTEPE), a value of 0.25 was used.

• Relativistic spin effects have been included in nuclear elastic scattering for accurate calculations near high Z interfaces.

•The electron step algorithm PRESTA-II (an essential requirement for accurate high–Z interface simulations) and the exact boundary crossing algorithm BCA PRESTA-I were also implemented.

Monte Carlo Calculations of the Photon Beam (2)

•A "Parallel Circular Beam with 2-D Gaussian X-Y Distribution" was used as the source type of incident electron beam in the BEAMnrc code. The value of FWHM of the Gaussian distribution was set to 2 mm.

• The energy spectrum of the electron beam was set from 2.3 to 6.25 MeV.

• A Tungsten target of 6mm diameter and 1 mm thickness was put as the e^-/X conversion unit.

•The influence of different energy spectra of electrons was then investigated.

,

Monte Carlo Calculations of the Photon Beam (3)

•Phase space files (PHSP) were generated for scoring planes at different distances from the tungsten target. The PHSP contain data relating to particle position, direction, charge, etc. for every particle crossing a scoring plane.

• The BEAMDP program was used for processing phase space files and to derive spectral distribution, mean energy distribution and fluence versus position of a photon beam in air.

• The following figures show the energy spectrum and the fluence versus position of a photon beam for a field area with a radius of 10 cm, at a distance of 100 cm from the tungsten target.

• Photon fluence is normalised by the energy bin width, number of incident particles, and the area of the field being considered. The mean energy of photon beam changes was from 1.18 MV to 1.14 MV, at a distance of 10 cm from the beam axis.

,

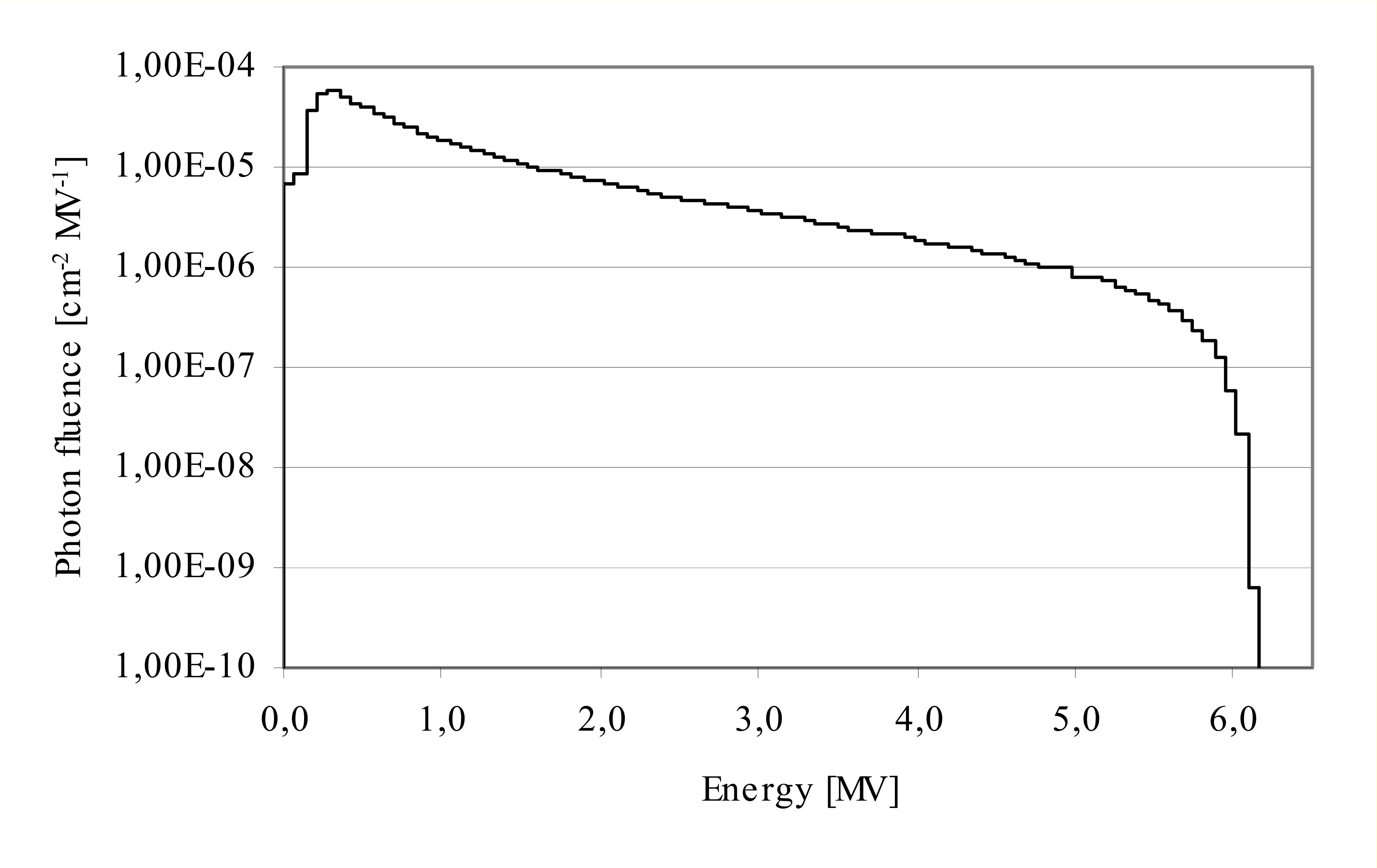

Energy spectrum of a photon beam in air for the field area with a radius of 10 cm at a distance of 100 cm from the tungsten target.

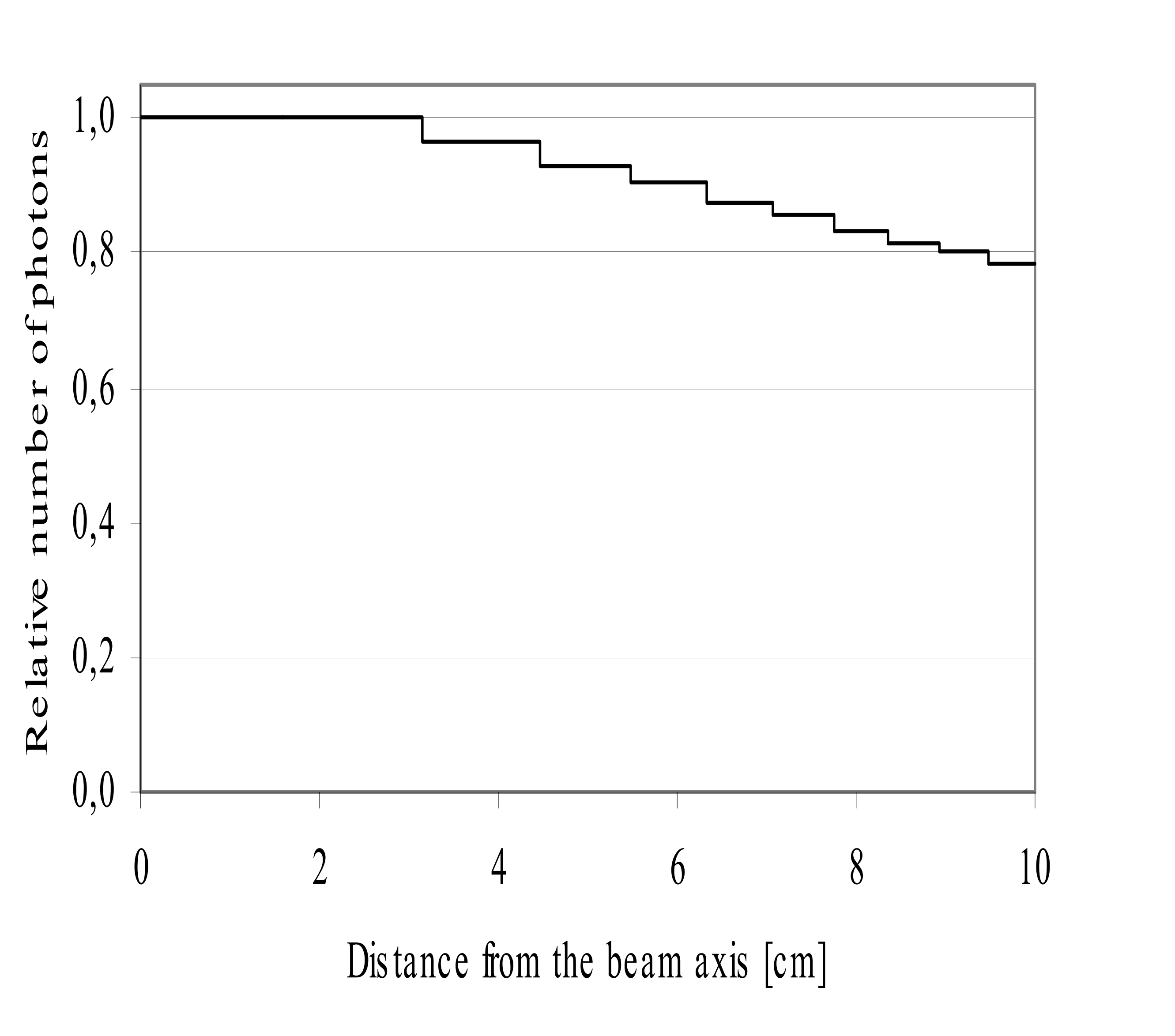

Fluence versus position of a photon beam in air for the field area with a radius of 10 cm at a distance of 100 cm from the tungsten target.

,

Radiographic Pictures

- Kodak Industrex AA 400 film was chosen for radiographic images.
- Experiments with different exposures and filters were performed to obtain the good radiographic contrast. 0.2 mm, front and back Pb screens were used.
- Flaw detectability: 0.4% for 10 cm thick steel object.

Radiographic image of the diode electron gun

,

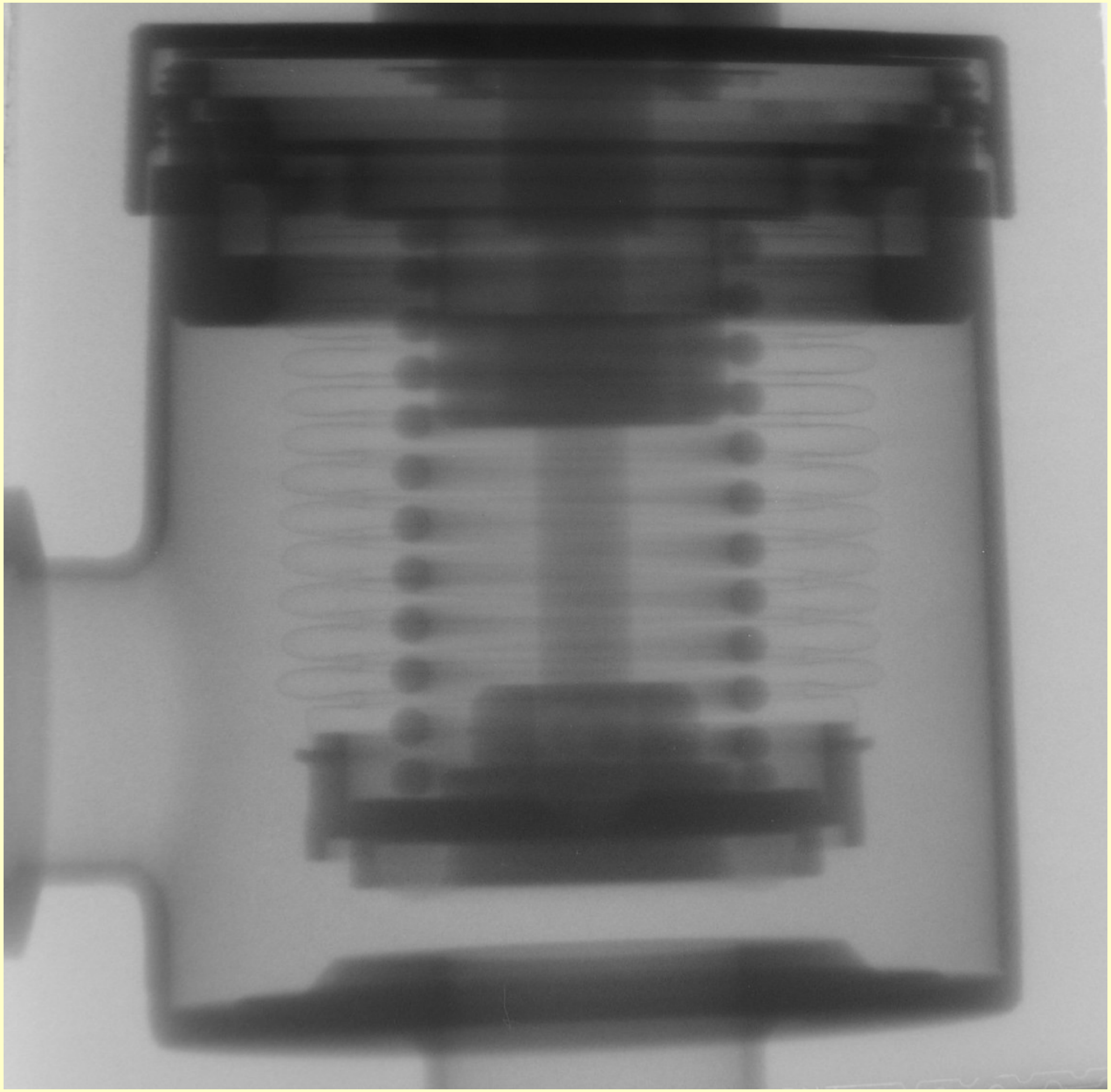

Radiographic image
of the vacuum valve

,